Effect of turbulent Schmidt number on the scalar field simulation of a fluidic precessing jet flow

†Xiao Chen, *Zhao Feng Tian and Graham 'Gus' Nathan

[1]Center for Energy Technology,
The School of Mechanical Engineering
The University of Adelaide, Adelaide, SA 5005, Australia

*Presenting author, † Corresponding author: xiao.chen01@adelaide.edu.au

Abstract

A preliminary numerical study of the external scalar field of a fluidic precessing jet (FPJ) flow is reported. The unsteady Shear Stress Transport (SST) model, which showed generally good agreement with the measured velocity field of flows within a FPJ nozzle, despite some discrepancies, was adopted to assess the effect of the turbulent Schmidt number, Sc_t, on the simulated scalar field. The simulated jet axis concentrations with three turbulent Schmidt number values, Sc_t =0.5, 0.9 and 1.3 have been compared with the measured results in the literature. It is found that the SST model over-predicts the centreline concentration of the jet in the near field downstream from the exit of the FPJ nozzle, while under-predicts it in the far field. An increase in Sc_t number causes the simulated jet to be more distributed away from the axis of the confinement, which is in contrast to the measured data. The best agreement with the measured result was achieved by adopting a Sc_t number of 0.5. However, due to the complexity of the FPJ flow, it is not feasible for a two-equation URANS model to reliably reproduce the scalar field by simply adjusting the turbulent Schmidt number.

Keywords: scalar mixing, turbulent Schmidt number, CFD, URANS

Introduction

A fluidic precessing jet (FPJ) nozzle, which has been employed in industrial rotary kilns was proposed by Nathan [1] to generate the FPJ flow. Numerous previous investigations of the flows within the FPJ nozzle have conducted by experimental measurements [2, 3], analytical method [4] and recently computational fluid dynamics (CFD) [5, 6]. Compared with the many studies of flows within the FPJ nozzle, the study of scalar mixing downstream the FPJ nozzle is much less. Parham [7] and Parham et al. [8] measured the scalar field downstream the FPJ nozzle using a two colour planar laser-induced fluorescence technique. In these studies, the effects of co-flow, confinement and a shaping jet on the mixing characteristics are investigated. Nevertheless, a reliable CFD model of the scalar field downstream the FPJ nozzle is still lacking. Hence the main objective of this paper is to preliminarily assess the feasibility of the unsteady Reynolds-Averaged Navier-Stokes (URANS) turbulence model in predicting the scalar field of the FPJ flow.

In the previous CFD studies of the flows within the FPJ nozzle [5, 6] conducted in the authors' group, the authors have assessed the performance of the Shear Stress Transport (SST) model in modeling the turbulent flows within the FPJ nozzle. The SST model achieves reasonable agreement with the measured mean axial velocity profiles for pipe and contraction inlets [6], and the measured centerline velocity decay and equivalent diameters of the phase-averaged precessing jet for the contraction inlet case despite some discrepancies [5]. Therefore the current CFD model of the scalar field downstream the FPJ nozzle is based on the SST model.

When applying the URANS models for the scalar field simulation, the turbulent Schmidt number (Sc_t), which is defined as the ratio of the turbulent eddy viscosity (μ_t) and the turbulent diffusivity (Γ_t), was found to have great influence on the simulated turbulent mixing [9]. In a numerical simulation of a jet in a cross-flow simulated with the standard k-ε model [10], the range of the turbulent Schmidt number, from 0.5 to 0.9, was found to have slight influence on the simulated temperature field. In another study of temperature field in a cross-flow [11], it was also found that the simulated temperature distribution is not sensitive to the turbulent Schmidt number. However, it is found that the turbulent Schmidt number has a significant influence on the simulated scalar mixing and Sc_t =0.2 is recommended for the simulation of a jet in a cross-flow [11]. Nevertheless, how the turbulent Schmidt number will influence the simulated scalar mixing of a FPJ flow is unclear.

The main aim of the current paper is to assess the effect of turbulent Schmidt number on the simulated scalar field in a flow downstream a FPJ nozzle. The FPJ flow investigated in [7, 8] are simulated using the SST model. The simulated jet concentration based on the turbulent Schmidt number, Sc_t =0.9, is compared with measured values reported in [7]. The default value of the turbulent Schmidt number is normally set as 0.9 (e.g. in ANSYS/CFX and ANSYS/FLUENT). A lower Sc_t number of 0.5 is tested in the current study following the work [10], and a larger Sc_t number of 1.3 is also tested.

Numerical Model

ANSYS/Designmodeler 16.5 was used to generate the 3-dimensional CFD geometry. Figure 1 illustrates geometric configuration of the CFD domain that includes an FPJ nozzle with a contraction inlet and a confinement. This geometry is identical to the configuration in the experimental studies [7]. The confinement is a cylindrical domain which has a diameter of 390 mm and a length of 1100 mm. The FPJ nozzle has a length of 115 mm from the main flow inlet to the exit of the contraction and 110 mm from the contraction exit to the nozzle exit. The inner diameter of the FPJ nozzle is 38 mm and the diameter of the center body is 27 mm. More details of the FPD nozzle can be found in the literature [7].

Figure 2 presents the details of the CFD mesh that was generated with the software ANSYS/ICEM CFD 16.5. The O-grid method was adopted to generate the structured mesh to

ensure the mesh quality, especially in the near wall region, which makes the y+ values to be less than 1. A mesh independent test has been conducted and a final mesh of 8.6 million nodes is used for the study.

The CFD software ANSYS/CFX 16.5 was adopted for the simulations. The flow of the CFD model is a multiple component fluid that includes two fluids. Water at 25 °C was employed as the first fluid (fluid1). A second fluid (termed as fluid2 in the model) is used for the co-flow, while its properties are exactly the same as those of the fluid1 at the main inlet. This numerical approach matches the experiment [7,8] in which the jet fluid was water marked with a fluorescent dye. The dye in the experiment is with very low concentration and its effects on the water dynamic properties can be neglected. At the main flow inlet (see Figure 1b), mass fraction of fluid1 is 1, i.e. the mass fraction of fluid2 is 0. At the co-flow inlet, mass fraction of fluid1 is 0 and the mass fraction of fluid2 is 1.

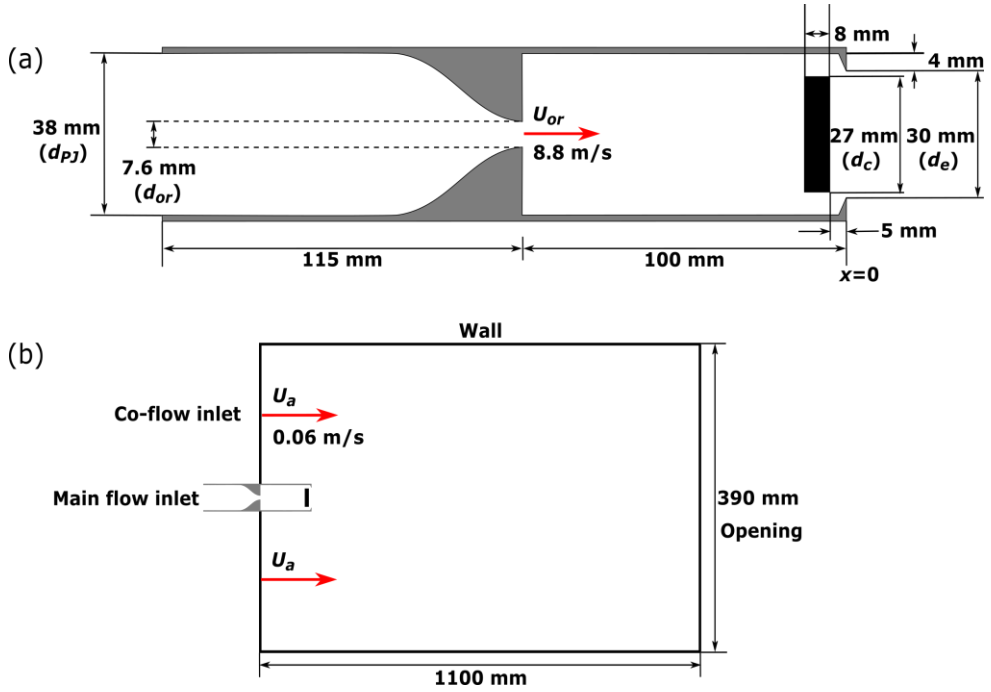

Figure 1: The geometric configurations of (a) the FPJ nozzle and (b) the whole fluid domain. Here d_{PJ}, d_{or}, U_{or} and U_a are the diameter of the nozzle, diameter of the inlet orifice, the inlet velocity at the orifice and the co-flow velocity, respectively.

For multi-component gases, the continuity equation and momentum equation after Reynolds averaging [12] are given as below:

$$\nabla \cdot U = 0 \tag{1}$$

$$\frac{\partial(\rho U)}{\partial t} + \nabla \cdot (\rho UU) = -\nabla p + \nabla \cdot \left\{ \mu \left[\nabla U + (\nabla U)^T \right] - \rho \overline{UU} \right\} + S_M \tag{2}$$

here U is the mean velocity vector, P the mean pressure, S_M the external momentum source, and ρ the mixture density that is calculated as:

$$\rho = \sum_{I=1}^{Nc} Y_I \rho_I \tag{3}$$

where ρ_I is the density of the component I. *Nc* is the number of modelled species in the mixture, and Y_I is the mass fraction of the species I that is solved by the following equation:

$$\frac{\partial(\rho Y_I)}{\partial t} + \nabla \cdot (\rho U Y_I) = \nabla \cdot (\Gamma_{I.eff} \nabla Y_I) + S_I \quad (4)$$

here S_I is the source term of the species. The effective diffusion coefficient of species I, $\Gamma_{I.eff}$, in Equation 4 is calculated as [12]:

$$\Gamma_{I.eff} = \Gamma_I + \frac{\mu_t}{Sc_t}, \quad (5)$$

Where Γ_I is the molecular diffusion coefficient of species, $\Gamma_I = \rho_I D_I$, D_I the kinematic diffusivity of the species I, μ_t the turbulent viscosity.

The root mean square (r.m.s) residuals are all under 5 x 10^{-5}. The high resolution scheme and the second order backward Euler scheme were adopted for the advective and transient terms, respectively.

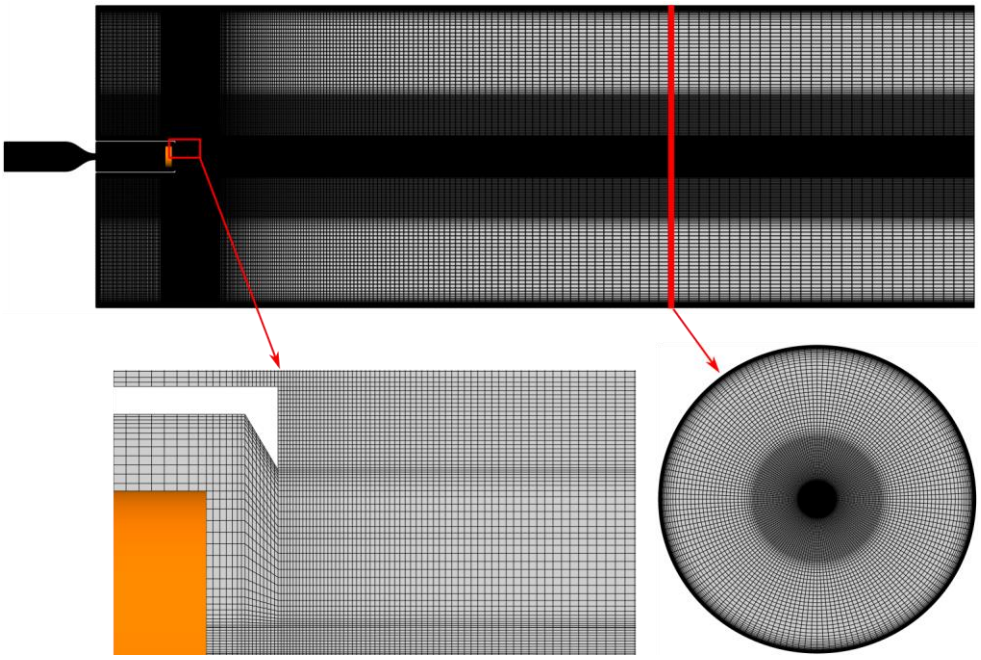

Figure 2: Mesh of the CFD model.

Preliminary Results and Discussion

Figure 3 compares the measured [7] and simulated instantaneous concentration of the jet on a cross-sectional plane downstream the nozzle exit with the Sc_t value of 0.5, 0.9 and 1.3, respectively. It can be seen that the small eddies and scalar concentration fluctuation in the measured instantaneous flow have not been reproduced with any of the three URANS approaches. The three simulated deflected angles between the instantaneous jets and the nozzle axis (indicated as the dashed lines) are similar, although they all appear to be larger than the measured data. It is observed that the value of Sc_t does not have a significant influence on the simulated flows within the FPJ nozzle. This observation can be explained by reviewing equations 1-4 and the inlet conditions in the flow. The turbulent Schmidt number is

only incorporated in Equations 4, which describes the transport of mass fraction of species. That is, it influences only the mixture density (Equation 3) and then the mixture flow field (Equations 1 and 2). If there is no mixing process, i.e. the mass fraction of a species is 1, the change of Sc_t will effect neither the mixture density nor the mixture species field. In the current case, the mass fraction of fluid1 is 1 at the main flow inlet and is nearly 1 anywhere inside the FPJ nozzle, except in a small region near to the nozzle exit where the mixture in the emerging field can be entrained into the FPJ nozzle. Nevertheless, as shown in Figure 4, the mass fraction of the mixture entrained into the FPJ nozzle exit region is very small and can be neglected.

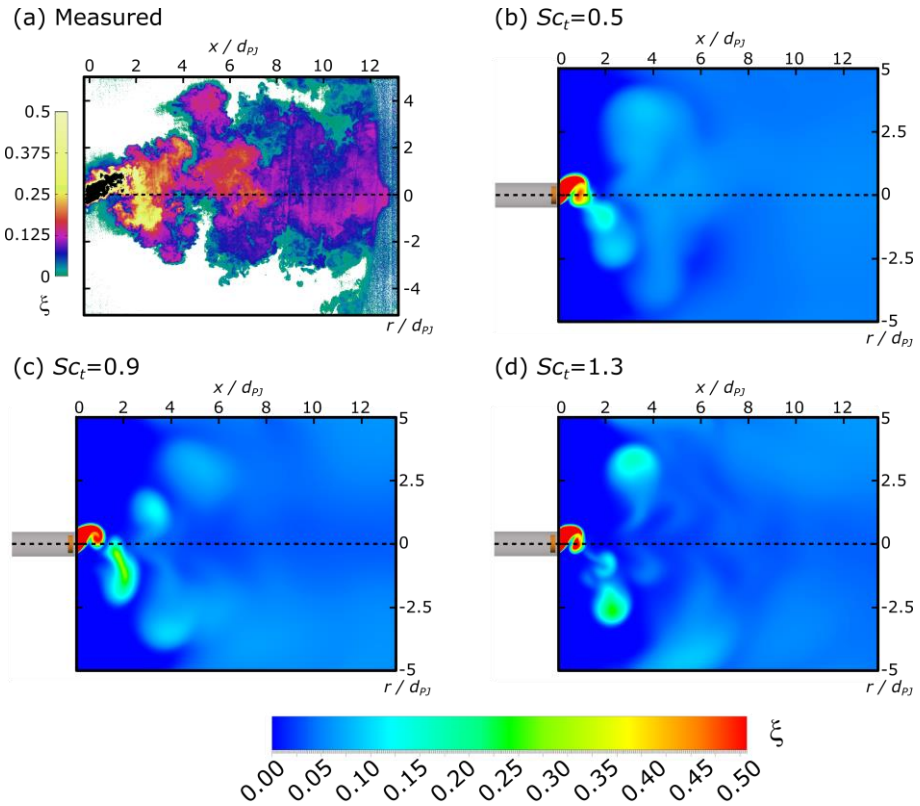

Figure 3: Instantaneous concentration cross-sectional contours of the FPJ flows that were (a) measured [7] and simulated using the SST model with the Sc_t value of (b) 0.5, (c) 0.9 and (d) 1.3.

The effect of the turbulent Sc_t number on the mixing process within the external flow is more pronounced than within the chamber, as is shown in Figure 3b-d. It can be seen that when the turbulent Sc_t number increases from 0.5 to 1.3, the diffusion of the fluid1 in the external flow decreases, leading to higher conentration of fluid1 in some flow vortexes. This can be explained by looking at Equation 5, when the turbulent Sc_t number increases, the effective diffusion coefficient of species I decreases, leading to lower diffusion of fluid1 as shown in Equation 4.

Figure 5 compares the measured [7] and simulated centreline concentration with three turbulent Schmidt numbers, namely, Sc_t = 0.5, 0.9 and 1.3. The measured centerline concentration of the jet exhibits a fast decay in the region from the FPJ exit (x/d_{PJ}=0) to an

"elbow point" (x/d_{PJ}≈1.4). At the "elbow point", the decay rate suddenly decreases and is nearly constant downstream from that point. This trend has been simulated with all the three models, however, the distance between the "elbow point" and the nozzle exit is over-predicted. For all CFD cases, the centreline jet concentration is over-predicted in the emerging field (say x/d_{PJ}<0.5) and is under-predicted in the region downstream from about x/d_{PJ}=1, especially in the region near to the "elbow point".

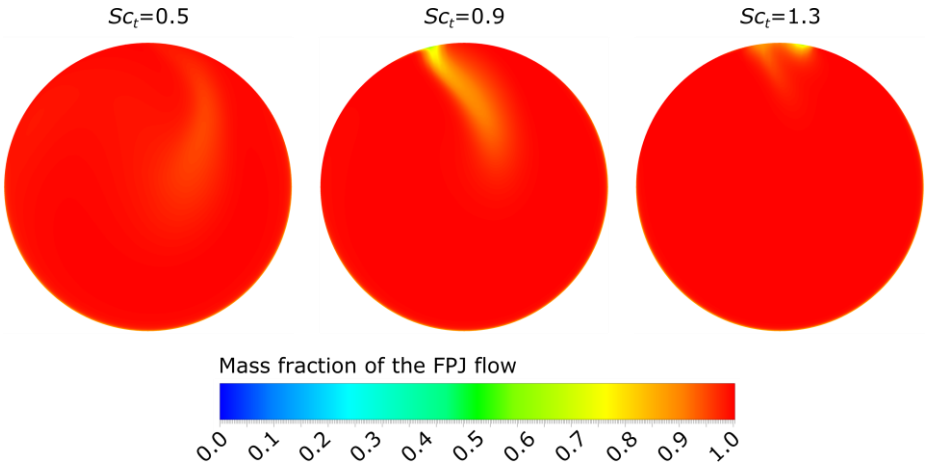

Figure 4: Instantaneous concentration contours of the Fluid1 on the nozzle exit (x=0) that were simulated using the SST model with the Sc_t value of 0.5, 0.9 and 1.3.

Figure 5 also shows that a decrease in Sc_t number leads to a decrease in centreline concentration, indicating a higher simulated mixing in the near field (x/d_{PJ}<0.5). This is consistent with Equations 4 and 2 that a decrease in Sc_t number causes the effective diffusivity to increase, hence improves the simulated scalar mixing. However in the far field (x/d_{PJ}>1), model with the lowest Sc_t number (Sc_t=0.5) simulated the highest centreline jet concentration. One possible reason is that, based on the observation of the simulated instantaneous jet concentration, the jet flow was simulated to be distributed preferentially in the near wall region as the increase of Sc_t number. Although the best agreement against the measured data was achieved by adopting a turbulent Schmidt number of 0.5, this model greatly under-predicts the centreline concentration of the jet in the region near to the "elbow point" (x/d_{PJ}≈1.4). This implies that the mechanism is not one of "turbulent" diffusion, but is rather controlled by the exit angle of the emerging jet, which is a function of large scale turbulent flow features.

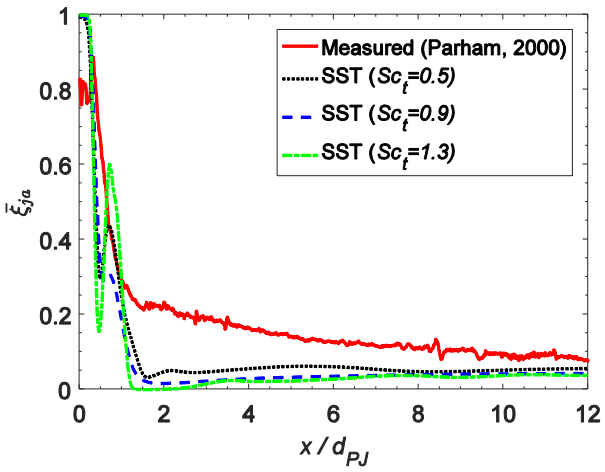

Figure 5: Measured [7] and simulated mean centerline concentration of the jet.

Summary

A decrease in Sc_t number causes the centreline concentration of the FPJ flow to decrease in the emerging field and increase in the far field. However, all the three approaches are found to over-predict the centreline concentration of the jet in the emerging field downstream the exit of the FPJ nozzle while under-predict it in the far field. This is due to large-scale features of the turbulent flow rather than to small scale "diffusion" processes, which are modelled by the turbulent Schmidt number. For this reason, the level of disagreement between the measured and predicted values of the scale field is not improved by changes to the turbulent Schmidt number. Indeed, the trends are opposite to what would be expected.

The flow in the far field of the confined, co-flowing turbulent FPJ flow is simulated to be distributed mostly in the region near to the wall of the confining cylinder, while the measured jet is preferentially distributed near to the axis. This discrepancy between the simulated and measured scalar field may be attributed to the over-predicted angle of the jet emerging from the FPJ nozzle.

Acknowledgements

The first author was supported by the Divisional Scholarship of the faculty of ECMS, the University of Adelaide. The authors gratefully acknowledge the support of the Australian Research Council through Grant DP150102230.

References

[1] Nathan, G., 1988, "The enhanced mixing burner." PhD Thesis, the University of Adelaide.
[2] Nathan, G., Hill, S., and Luxton, R., 1998, "An axisymmetric 'fluidic'nozzle to generate jet precession," Journal of Fluid Mechanics, 370, pp. 347-380.
[3] Wong, C., Lanspeary, P., Nathan, G., Kelso, R., and O'Doherty, T., 2003, "Phase-averaged velocity in a fluidic precessing jet nozzle and in its near external field," Experimental Thermal and Fluid Science, 27(5), pp. 515-524.
[4] Kelso, R., 2001, "A mechanism for jet precession in axisymmetric sudden expansions." In the Proceeding of 14th Australasian Fluid Mechanics Conference, pp. 829-832.

[5] Chen, X., Tian, Z., Kelso, R., and Nathan, G., 2017, "The topology of a precessing flow within a suddenly expanding axisymmetric chamber," ASME Journal of Fluids Engineering, 139(7), 071201.
[6] Chen, X., Tian, Z. F., Kelso, R. M., and Nathan, G. J., 2017, "New understanding of mode switching in the fluidic precessing jet flow," ASME Journal of Fluids Engineering, 139(7), 071102.
[7] Parham, J. J., 2002, "Control and optimisation of mixing and combustion from a precessing jet nozzle," PhD thesis, the University of Adelaide.
[8] Parham, K., Esmaeilzadeh, E., Atikol, U., and Aldabbagh, L., 2011, "A numerical study of turbulent opposed impinging jets issuing from triangular nozzles with different geometries," Heat and Mass Transfer, 47(4), pp. 427-437.
[9] Reynolds, A., 1975, "The prediction of turbulent Prandtl and Schmidt numbers," International Journal of Heat and Mass Transfer, 18(9), pp. 1055-1069.
[10] Chao, Y.-C., and Ho, W.-C., 1991, "Heterogeneous and nonisothermal mixing of a lateral jet with a swirling crossflow," Journal of Thermophysics and Heat Transfer, 5(3), pp. 394-400.
[11] He, G., Guo, Y., and Hsu, A. T., 1999, "The effect of Schmidt number on turbulent scalar mixing in a jet-in-crossflow," International Journal of Heat and Mass Transfer, 42(20), pp. 3727-3738.
[12] Tian, Z. F., Witt, P. J., Schwarz, M. P., and Yang, W., 2018, "Numerical Modelling of Pulverised Coal Combustion," Handbook of Multiphase Flow Science and Technology, G. Yeoh, ed., SPRINGER Singapore.